JOURNAL OF APPLIED ELECTROCHEMISTRY 21 (1991) 915–921

Coupling between electrolysis and liquid-liquid extraction in an undivided electrochemical reactor: applied to the oxidation of Ce^{3+} to Ce^{4+} in an emulsion Part I. Experimental*

D. HORBEZ

Rhône-Poulenc — Centre de Recherches d'Aubervilliers, 52, rue de la Haie Coq, 93308 Aubervilliers, Cedex, France

A. STORCK

Laboratoire des Sciences du Génie Chimique, CNRS-ENSIC, 1, rue Grandville, BP451, 54001 Nancy, Cedex, France

Received 3 December 1990; revised 13 May 1991

The effect of *in situ* simultaneous extraction of tetravalent cerium by an organic phase (di-2 ethylhexylphosphoric acid in kerosene) on the performance of an undivided batch electrochemical reactor using the Ce^{3+}/Ce^{4+} system was investigated. The influence of the most important parameters (initial concentration of Ce^{3+}, composition and volume percentage of the organic phase) were studied experimentally under potentiostatic control of the anode potential. A conversion factor of Ce^{3+} and extraction factor larger than 90% are obtained for the best operating conditions, but the presence of the organic phase and the necessity of avoiding oxygen gas evolution considerably reduce the operating anodic current densities. The transient cell behaviour and the final "equilibrium" state conditions are found to be in very good qualitative agreement with the conclusions of a preliminary study of the electrochemical kinetics of the Ce^{3+}/Ce^{4+} system and extraction mechanisms of Ce^{4+} by the organic phase.

Nomenclature

A_e	electrode area (m^2)
C	concentration (M)
CF	conversion factor of Ce^{3+}
D	molecular diffusion coefficient ($m^2 s^{-1}$)
E	electrode potential (V)
E_0^0	standard potential of the Ce^{3+}/Ce^{4+} redox system (V)
EF	extraction factor
F	Faraday constant (96 485 A s mol^{-1})
i	current density ($A m^{-2}$)
I	current (A)
i_0	exchange current density ($A m^{-2}$)
k_0^0	standard electrochemical rate constant of the Ce^{3+}/Ce^{4+} system ($m s^{-1}$)
k_d	mass transfer coefficient (measured by electrochemical reduction of Ce^{4+} except Fig. 5) ($m s^{-1}$)
K_M	equilibrium constant of the extraction mechanism ($mol^2 l^{-6}$)
m	partition coefficient of tetravalent cerium
R	perfect gas constant ($J mol^{-1} K^{-1}$)
t	time (s)
T	temperature (K)
V	reactor volume (l)

Greek symbols

α	anodic charge transfer coefficient
β	cathodic charge transfer coefficient
ε	volumic organic phase ratio in the dispersion
η	overall current efficiency or overpotential (- or V)
ν_e	number of electrons involved in the electrochemical process (= 1)

Subscripts

a	anodic
c	cathodic
3	trivalent cerium
4	tetravalent cerium
0	at time $t = 0$

* This paper is dedicated to Professor Dr Fritz Beck on the occasion of his 60th birthday.

0021-891X/91 $03.00 + .12

1. Introduction

Electrochemical processes frequently require the use of divided reactors, using a diaphragm or a membrane, especially when the product of a reaction occurring at the working electrode may be re-oxidized or re-reduced at the counter electrode, the result being decrease of the overall operation efficiency. An interesting means of avoiding the use of separators, which has been rarely considered to date [1, 6], is the simultaneous extraction of the product by a selective, electrochemically inert, organic phase, dispersed in the aqueous phase. The Purex process [5, 6] for the separation of plutonium and uranium and the recent work of Pletcher [3, 4] related to the oxidation of aromatic compounds by Ce^{4+} in an emulsion system are specific examples of such a coupling between electrolysis and liquid-liquid extraction. The aim of this study is to present the results of an experimental (Part I) and theoretical analysis (Part II) of the behaviour of a batch undivided electrochemical reactor with regards to the electrochemical oxidation of Ce^{3+} to Ce^{4+}, extracted *in situ* by a dispersed phase of di-2 ethylhexylphosphoric acid D_2EHPA in kerosene (see Fig. 1). The potential interest of this operation lies, on the one hand, in the possibility of recovering cerium from a mixture of rare earths by changing its degree of oxidation [7] and, on the other hand, in the use of the oxidizing character of Ce^{4+} for indirect electroorganic synthesis [8].

The first part of this paper presents experimental results of the effect of several important parameters (initial concentration of Ce^{3+}, composition and volume percentage of the organic phase, electrode potential, etc.) on the performance (conversion factor of Ce^{3+}, extraction factor, current efficiency) of a batch reactor operated potentiostatically.

A simulation of the batch process based on mass and charge balances, adequate kinetic laws and mechanisms of liquid-liquid extraction of Ce^{4+} will be the subject of the second part of the paper.

2. Electrochemical kinetics of the Ce^{3+}/Ce^{4+} system and extraction mechanisms of Ce^{4+} by D_2EHPA

2.1. *Electrochemical kinetics*

2.1.1. Review of the literature. The anodic reaction investigated is the oxidation of Ce^{3+}: $Ce^{3+} \rightarrow Ce^{4+} + e^-$ whereas two cathodic reactions are considered: the back reduction of Ce^{4+} to Ce^{3+}, which should be minimized through selective extraction of Ce^{4+} and, in acidic medium, hydrogen evolution (see Fig. 1). The chosen electrolyte was sulphuric acid (in nitric acid, the cathodic reduction of nitrate ions has also to be considered [9]).

Analysis of the published kinetic and thermodynamic data of the Ce^{3+}/Ce^{4+} system leads to the following conclusions [10]:

— because of complex formation, the formal redox potential E_0^0 for cerium strongly depends on the electrolyte considered and $E_0^0 \simeq 1.44$ V/SHE in 0.5 M H_2SO_4 [11].

— in a sulphuric acid medium, trivalent cerium is present in two forms Ce^{3+} and $CeSO_4^+$, while the main form of tetravalent cerium is $Ce(SO_4)_3^{2-}$ [12, 13].

— according to the studies of Randle and Kuhn [14], at least two mechanisms should be considered for the anodic oxidation of trivalent cerium:

$$Ce^{3+} + SO_4^{2-} \longrightarrow Ce(SO_4)^{2+} + e^-$$

$$Ce\,SO_4^+ + SO_4^{2-} \longrightarrow Ce(SO_4)_2 + e^-$$

It should be mentioned that the high value of E_0^0 implies the choice of a corrosion resistant electrode material with a sufficiently high overvoltage for anodic

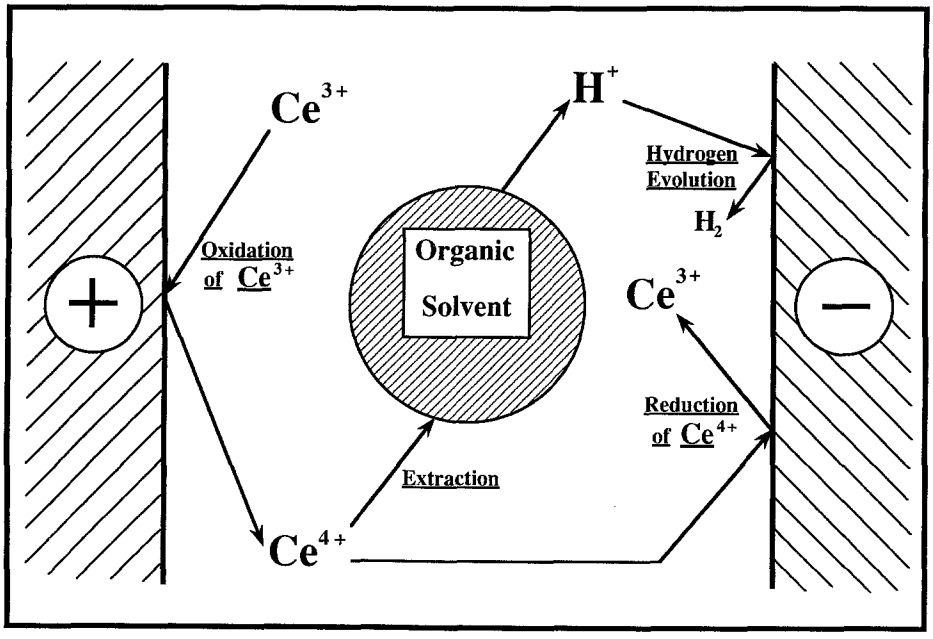

Fig. 1. Schematic representation of the coupling between electrolysis and liquid-liquid extraction (Ce^{3+}/Ce^{4+} system).

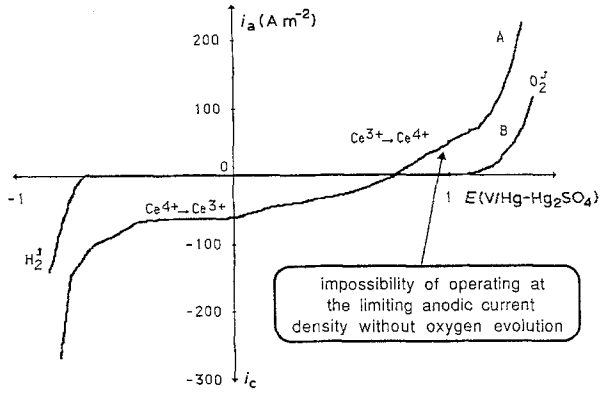

Fig. 2. Example of current-potential curves obtained with Ti/Pt electrodes in a laboratory cell (aqueous phase alone). Curve A: (Ce^{3+}) 7.5 × 10^{-3} M, (Ce^{4+}) 2.5 × 10^{-3} M, (H_2SO_4) 0.5 M; Curve B: (H_2SO_4) 0.5 M alone.

oxygen evolution, in order to minimize this unwanted reaction. Platinized titanium was therefore chosen for both cathode and anode.

2.1.2. Experimental results. Figure 2 shows a typical current-potential curve obtained in a 0.5 M H_2SO_4 medium on a Pt/Ti plate immersed in a laboratory cell. On the cathodic side, the reduction wave of Ce^{4+} presents a well defined limiting currenty density with hydrogen evolution for higher overpotentials. The shape of the current-potential plot may be due to the existence of different forms of tetravalent cerium. On the anodic side, curve B, obtained with H_2SO_4 0.5 M alone, shows that oxygen evolution is significant for potentials above 1.1 V/Hg-Hg_2SO_4 electrode. At this potential, which is a limit for avoiding oxygen gas evolution, and assuming that both anodic reactions occur independently, the current density for Ce^{3+} oxidation (curve A) represents only 12% of the calculated limiting current density for the Ce^{3+} concentration considered. Concerning the process design, oxygen evolution must be strictly avoided for two reasons: one due to the fact that hydrogen will be generated cathodically and the other from the point of view of the anodic current efficiency.

The value of 1.1 V is therefore an upper limit for the anodic potential, which consequently implies a strong limitation of the possible operating current density range.

Based on the analysis of the current-potential curves obtained on a platinized titanium plate in a laboratory cell or on a 3 mm platinum rotating disc electrode, both anodic and cathodic processes may be described, as a first approximation, by a simple Butler–Volmer equation including mass transfer limitations through the Nernst film model [10]. The corresponding cathodic and anodic current densities are then given by the following expressions:

$$\frac{|i_c|}{v_e F} = \left(k_0^0 C_4 \exp\left[-\beta \frac{v_e F}{RT}(E_c - E_0^0)\right] - k_0^0 C_3 \exp\left[\alpha \frac{v_e F}{RT}(E_c - E_0^0)\right]\right) \times \left(1 + \frac{k_0^0}{k_{dc}} \exp\left(-\beta \frac{v_e F}{RT}(E_c - E_0^0)\right) + \frac{k_0^0}{k_{dc}} \frac{D_4}{D_3} \exp\left[\alpha \frac{v_e F}{RT}(E_c - E_0^0)\right]\right)^{-1} \quad (1)$$

$$\frac{i_a}{v_e F} = \left(k_0^0 C_3 \exp\left[\alpha \frac{v_e F}{RT}(E_a - E_0^0)\right] - k_0^0 C_4 \exp\left[-\beta \frac{v_e F}{RT}(E_a - E_0^0)\right]\right) \times \left(1 + \frac{k_0^0}{k_{da}} \frac{D_4}{D_3} \exp\left(\alpha \frac{v_e F}{RT}(E_a - E_0^0)\right) + \frac{k_0^0}{k_{da}} \exp\left[-\beta \frac{v_e F}{RT}(E_a - E_0^0)\right]\right)^{-1} \quad (2)$$

For high absolute values of the cathodic or anodic overpotentials, these expressions may be linearized as follows:

$$\ln\left[\frac{|i_{CL}|\,|i_C|}{|i_{CL}| - |i_C|}\right] = \beta \frac{v_e F}{RT} |\eta_c| + \ln i_0 \quad (3)$$

$$\ln\left[\frac{i_{aL} i_a}{i_{aL} - i_a}\right] = \alpha \frac{v_e F}{RT} \eta_a + \ln i_0 \quad (4)$$

where the subscript 'L' refers to limiting current conditions.

Consequently, a plot of $\ln[(i_{aL} i_a)/(i_{aL} - i_a)]$ against η_a may lead to the anodic charge transfer coefficient α and exchange current density i_0. (A similar plot involving the cathodic current density i_c gives the cathodic charge transfer coefficient β).

From the present experimental results, the mean value $\beta = 0.2$ was obtained, in good agreement with most published data [14, 15, 16]. Concerning the anodic plots, it appears that α depends slightly on the bulk concentration of Ce^{3+}. As an example, Fig. 3 shows that α (~ 0.2) is a decreasing function of (Ce^{3+}). This phenomenon, already mentioned by Randle and Kuhn, can probably be explained by the formation of complex compounds between Ce^{3+} and SO_4^{2-} ions. In the simple Butler–Volmer equation considered here, only a single electrochemical mechanism is considered, while two forms of trivalent cerium are actually involved in the electron transfer. The participation of sulphate ions in both anodic and cathodic processes is also confirmed by the fact that $\alpha + \beta < 1$.

Finally, the standard rate constant k_0^0 obtained on platinized titanium in 0.5 M H_2SO_4 was found to be 2.1 × 10^{-6} m s^{-1} (ranging from 2 × 10^{-6} for the

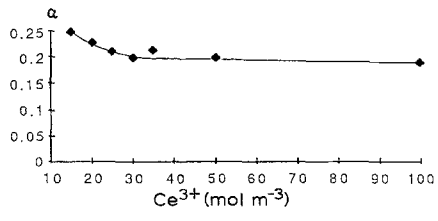

Fig. 3. Influence of the concentration of Ce^{3+} on the anodic charge transfer coefficient α (Rotating Pt disc electrode, H_2SO_4 1 M).

anodic current-potential curves to $2.2 \times 10^{-6}\,m\,s^{-1}$ for the cathodic curves).

2.2. *Extraction mechanisms of tetravalent cerium by D_2EHPA*

Di-2 ethylhexylphosphoric acid was selected as a possible extraction solvent in a sulphuric acid medium, because it is one of the most suitable compounds for the extraction of Ce^{4+} in terms of partition coefficient, selectivity, kinetics, chemical and electrochemical resistance and low solubility in the aqueous phase. Diluted in kerosene, it is mainly present as the dimeric form, noted $(D_2EHPA)_2$ and does not fix the sulphate ions [17]. Most authors consider the dimeric form exchanging one proton, leading to the following mechanism:

$$Ce^{4+} + 4\overline{(HA)}_2 \longrightarrow \overline{CeH_4A_8} + 4H^+$$

with D_2EHPA = HA. (The overlined species correspond to the organic phase).

From this equation the extraction of one tetravalent cerium requires 8 molecules of D_2EHPA.

However, there is experimental evidence (see, for example, Baes [18], Ritcey [19] and Horbez [10]) that this simple extraction mechanism does not exactly correspond to reality and that it is possible to extract more cerium than given by this stoichiometry; indeed the dimeric form may also exchange its second proton, leading to another possible mechanism:

$$Ce^{4+} + 2\overline{(HA)}_2 \longrightarrow \overline{CeA_4} + 4H^+$$

Nevertheless, consideration of these two simple mechanisms cannot satisfactorily explain the experimental results, especially as concerns the partition coefficient of Ce^{4+} between the two phases for various Ce^{4+} and D_2EHPA concentrations. With regards to the work of BAES for the extraction of UO_2^{2+}, we also suggest that there might be a progressive transition between both stoichiometries, explained in the case of uranyl ion by polymer formation, so that for a large excess of solvent the extraction would require $4D_2EHPA$ dimers, while only two are needed for lower concentrations.

In the simple approach considered in this work, the simplified second mechanism characterized by the equilibrium constant,

$$K_m = \frac{(\overline{CeA_4})(H^+)^4}{(Ce^{4+})(\overline{HA})_2^2} = m\frac{(H^+)^4}{(\overline{HA})_2^2}$$

has been considered where m is the partition coefficient of tetravalent cerium between the phases. From the previous discussion, K_m appears as a "hypocritical constant" [20], depending on the concentrations of the species involved in the extraction and which can be correlated to these concentrations.

3. Coupling between electrolysis and liquid-liquid extraction in a batch undivided cell

3.1. *Experimental apparatus and operating conditions*

The laboratory scale batch reactor designed for this study was a 0.75 dm^3 cylindrical glass reactor represented schematically in Fig. 4.

The electrodes were made of cylindrical platinized expanded titanium grids; the cathode was pressed against the wall of the cell, whereas the anode (made of two attached grids) was located between the central stirrer (standard Rushton turbine) and four baffles. This device was particularly well suited to maintaining a good dispersion of the organic phase, achieving low mass transfer rates at the cathode (in order to limit the reduction of Ce^{4+}) and high anodic mass transfer rates (in order to favour the oxidation of Ce^{3+}). The experimental variations of the mass transfer coefficients, k_d, measured with the classical $Fe(CN)_6^{3-}/Fe(CN)_6^{4-}$ redox system, with the stirring rates are shown in Fig. 5, which shows that, as expected, k_{da} is much higher than k_{dc}.

Moreover, the reactor geometry gave an anodic area slightly higher than the cathodic area (A_{ea} = 0.073 m^2; A_{ec} = 0.049 m^2; A_{ea}/A_{ec} = 1.48), which was of interest for increasing the cathodic current,

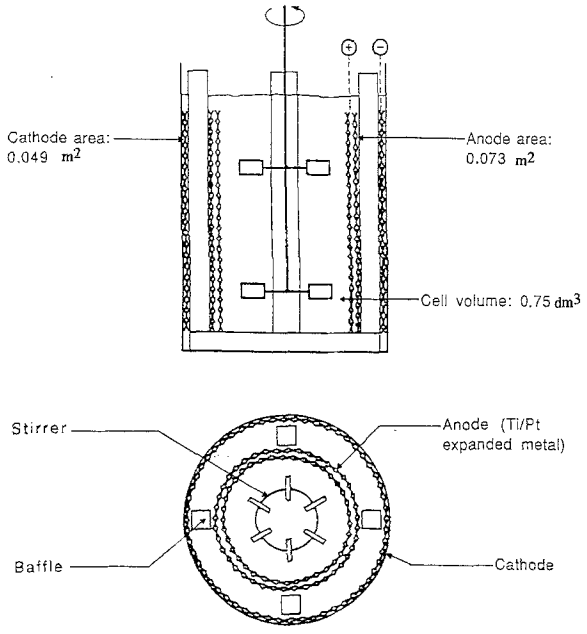

Fig. 4. Schematic view of the batch stirred tank electrochemical reactor.

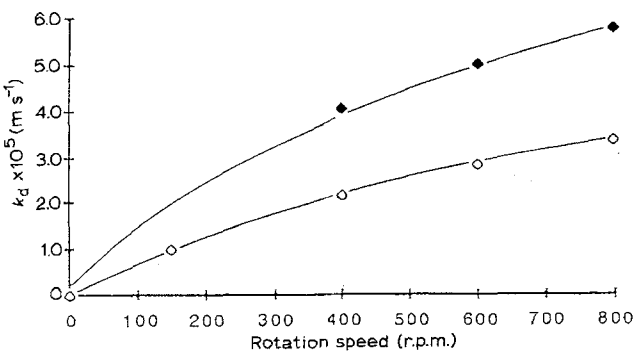

Fig. 5. Influence of the stirrer rotation speed on the anodic and cathodic mass transfer coefficient. (Temperature: 25 °C; aqueous phase: $Fe(CN)_6^{3-}/Fe(CN)_6^{4-}$ in 0.5 M NaOH). (◆) Anode; (◇) cathode.

efficiency with respect to hydrogen evolution. However, it has been shown that this effect was only really significant for ratios A_{ea}/A_{ec} greater than 10 [21].

The experiments were performed under potentiostatic control (E_a = 1.78 V/SHE to avoid oxygen evolution), using a mercury sulphate reference electrode located near the anode.

The investigated parameters were the volume ratio of organic phase in the dispersion ε, the initial D_2EHPA concentration in the organic phase and the initial Ce^{3+} and H_2SO_4 concentrations in the aqueous phase. During electrolysis, Ce^{3+} was electrochemically oxidized to Ce^{4+} which was partially extracted by the organic phase, while simultaneous hydrogen evolution and reduction of Ce^{4+} occurred at the cathode. The concentrations of Ce^{3+} and Ce^{4+} varied in time until an equilibrium was reached where $I_{Ce^{3+}\rightarrow Ce^{4+}} = I_{Ce^{4+}\rightarrow Ce^{3+}}$ and $I_{H_2} = 0$. At this equilibrium, the following figures of merit are defined for the process:

– the conversion factor of Ce^{3+}:

$$CF = 1 - (C_3/C_{30}) \quad (5)$$

– the extraction factor:

$$EF = [\varepsilon/(1 - \varepsilon)](\overline{C_4}/C_{30}) \quad (6)$$

– the partition coefficient of tetravalent cerium:

$$m = (\overline{C_4}/C_4) \quad (7)$$

– an overall current efficiency:

$$\eta = (1 - \varepsilon)V(C_{30} - C_3)F \Big/ \int_0^t I\,dt \quad (8)$$

3.2. *Results and discussion*

A summary of the most important experimental results obtained at equilibrium is presented in Table 1. The first line corresponds to a classical electrolysis performed in an aqueous phase (0.5 M H_2SO_4, C_{30} = 0.1 M) without simultaneous extraction of Ce^{4+} and the conversion factor of Ce^{3+} at equilibrium is only 23% (corresponding to C_3 = 0.077 M and C_4 = 0.023 M). The other results, all obtained with *in situ* extraction of tetravalent cerium by D_2EHPA, show a significant increase in the conversion, which reached 98% in the best operating conditions. This clearly demonstrates the feasibility and excellent performance of the coupling between electrolysis and extraction of the product.

3.2.1. Influence of the volume ratio of the organic phase. The influence of the volume percentage ε of the organic phase in the dispersion on the conversion and extraction factors is shown in Fig. 6 for an aqueous phase initially containing 0.5 M H_2SO_4 and 0.1 M Ce^{3+} and for a D_2EHPA concentration in the organic phase of 0.8 M. The curve clearly shows the favourable effect of an increase of ε up to 66%. However, it should be mentioned that the dispersion of such a concentrated emulsion is difficult, due to the sharp increase of the viscosity and the risk of phase inversion. Optimum values of ε (also taking into account the necessity of maintaining a good electrical conductivity) are, therefore, in the range 33–50%, where the conversion factors range from 85 to 90%.

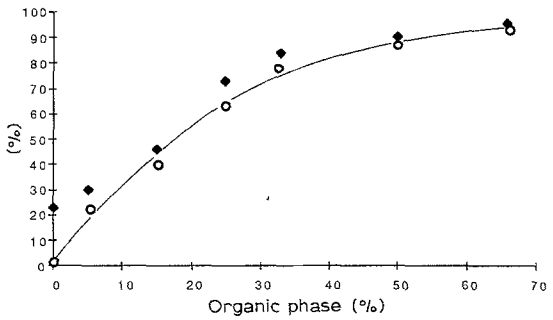

Fig. 6. Influence of the volumic percentage ε of the organic phase on the conversion and extraction factors of cerium at equilibrium. Aqueous phase: $(H_2SO_4)_0$ 0.5 M, $(Ce^{3+})_0$ 0.1 M; organic phase: $(D_2EHPA)_0$ = 0.8.M. (◆) Conversion factor; (O) extraction factor.

3.2.2. Influence of the initial D_2EHPA concentration in the organic phase. The extraction of high amounts of Ce^{4+} in the case of concentrated Ce^{3+} solutions requires significant quantities of D_2EHPA. However, solvent concentration was limited to 2 M (Pure D_2EHPA corresponds to approximately 3 M) since a high viscosity of the organic phase may lead to hydrodynamic problems. Figure 7 presents the effect of the initial D_2EDPA concentration on the conversion and extraction factors for the same conditions of Fig. 6 and for ε = 0.25. As can be seen, these two factors are increasing functions of $[D_2EHPA]_0$ at least up to 0.8 M. For higher concentrations, the difficulty of maintaining a good dispersion may explain the decrease of EF and CF.

Whereas values of EF and CF higher than 90% can be achieved in the best operating conditions, the very low values of the current densities constitute the weak point of the process, indeed, the initial anodic current density, as well as the equilibrium one, is always smaller than 70 A m^{-2} (obtained in the most favourable conditions). Three reasons can be proposed for explaining this fact:

– the low solubility of cerous sulphate, approximately

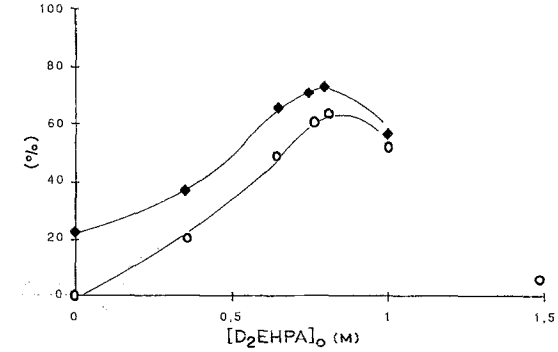

Fig. 7. Influence of the initial concentration of the extraction agent in the organic phase on the conversion and extraction factors of cerium at equilibrium. Aqueous phase: $(H_2SO_4)_0$ 0.5 M, $(Ce^{3+})_0$ 0.1 M; organic phase: ε = 25%. (◆) Conversion factor; (O) extraction factor.

Table 1. Summary of main experimental results obtained under potentiostatic control

$(Ce^{3+})i$ (M)	H_2SO_4 normality	Organic phase (%)	(D_2EHPA) (M)	Conversion factor at equilibrium (%)	Extraction factor at equilibrium (%)	Partition coefficient at equilibrium	$(Ce^{4+})org$ at equilibrium (M)	Anodic current density at $t = 0$ ($A\,m^{-2}$)	Current density at equilibrium ($A\,m^{-2}$)	Current efficiency at equilibrium (%)
0.1	1	0	–	23.0	0	–	–		44.0	
0.1	1	25	0.8	73.0	64.0	20.0	0.193	34.1	16.6	40
0.1	1	33	0.8	83.3	77.3	26.0	0.155	24.5	9.5	69
0.1	1	50	0.8	90.5	88.5	41.4	0.081	10.9	3.7	81
0.1	1	66	0.8	95.6	95.2	125.0	0.048	10.9	1.6	88
0.2	1	50	0.8	91.0	84.0	11.2	0.168	38.1	14.7	63
0.2	1	50	1.2	98.0	95.5	40.0	0.191	34.1	6.4	77
0.2	2	33	2.0	93.7	88.2	32.0	0.353	104.0	8.2	70
0.2	2	50	0.8	85.5	70.0	4.3	0.139	73.5	33.7	52
0.2	2	50	2.0	95.0	92.0	38.0	0.184	35.4	6.5	75

0.2–0.25 M at 25 °C (the solubility decreases with increasing temperature).

- the necessity of avoiding oxygen evolution limits the anode potential and also the anodic current density i_a, strongly controlled by activation electrode phenomena (in most cases, i_a represents less than 10% of the limiting current density).
- the strong decrease of the electrochemical rate constant, k_0^0, under the influence of the organic phase. As an example, it was found that $k_0^0 = 2.1 \times 10^{-6}\,m\,s^{-1}$ with the pure aqueous phase (see above), and with a 33% 0.8 M D_2EHPA organic phase, k_0^0 is reduced to $3.5 \times 10^{-7}\,m\,s^{-1}$. Adsorption phenomena at the anode may explain this fact.

Due to the different mechanisms of liquid-liquid extraction based on cationic exchange discussed above, higher D_2EHPA concentrations and lower acidities in the aqueous phase should lead to a larger partition coefficient, m, which is effectively confirmed by the experimental results at equilibrium shown in Table 1, for a given initial concentration of Ce^{3+} (second part of Table 1). Finally, all experimental results obtained at equilibrium in the batch undivided electrochemical reactor are in good qualitative agreement with the conclusions deduced from the preliminary study of the electrochemical kinetics for the Ce^{3+}/Ce^{4+} system and extraction mechanisms with D_2EHPA. The transient behaviour of the cell before reaching equilibrium is the subject of Part II of this work, as well as the comparison between experimental and calculated results. Qualitatively, the concentration of Ce^{3+} decreases with time, until it reaches its equilibrium value, whereas the (Ce^{4+}) concentration in the aqueous phase increases slowly. The observed decrease of the current density may be explained by considering the general form of the Butler–Volmer equation and the linear influence of (Ce^{3+}). The partition coefficient, m, also decreases during electrolysis as a consequence of the effects of D_2EHPA concentration and acidity of the aqueous phase, which were discussed above.

4. Conclusions

This experimental work has shown that the coupling between electrolysis and liquid-liquid extraction in the case of Ce^{3+} oxidation with simultaneous extraction of tetravalent cerium, allows a quantitative conversion of Ce^{3+} with reliable current efficiencies which would not be obtained in a classical undivided cell operated with a single aqueous phase. However the low operating current densities imposed by the necessity of avoiding oxygen evolution and the strong decrease of the electrochemical rate constant due to the organic phase certainly constitute the weak point of a potential process where three dimensional electrodes might be used in order to compensate the low current densities by high interfacial electrode areas.

Acknowledgement

The authors acknowledge the financial support of this work by Rhône-Poulenc (France) and Messrs Grosbois and Feltin for fruitful discussions.

References

[1] S. Zhang and D. Deng, *He Yuaxue Yu Fangshe Huaxue*, **4**(4) (1982) 243–8.
[2] Y.-S. Shih and J.-L. Lee, *J. Appl. Electrochem.* **17** (1987) 480–8.
[3] D. Pletcher and E. M. Valdes, *Electrochim. Acta* **33** (1988) 499–507.
[4] *Idem., ibid.* **33** (1988) 509–15.
[5] H. Feess and H. Wendt, *Chem. Ing. Tech.* **53** (1981) 808–9.
[6] N. L. Weinberg and B. V. Tilak, 'Techniques of electroorganic synthesis', Part III, Wiley Interscience, New York (1982) chap. 2, pp. 168–70.
[7] T. Sekine and Y. Hasegawa, 'Solvent extraction chemistry, fundamentals and applications', Marcel Dekker, New York (1977).
[8] E. Steckhan, *Topics in current chemistry* **142** (1987) 1–69.
[9] M. Martin and A. Rollat, European Patent 0 198 736 (1986).
[10] D. Horbez, Thesis, Institut National Polytechnique de Lorraine, September 1988.
[11] A. H. Kuntz, *J. Am. Chem. Soc.* **53** (1931) 98–102.
[12] T. J. Hardwick and E. Robertson, *Canad. J. Chemistry* **29** (1951) 828–37.

[13] T. W. Newton and G. M. Arcand, *J. Am. Chem. Soc.* **75** (1953) 2449–53.
[14] T. H. Randle and A. T. Kuhn, *J. Chem. Soc. Faraday Trans.* 1 **79**, 8 (1983) 1741–56.
[15] Z. Galus and R. N. Adams, *J. Phys. Chem.* **67** (1963) 866–71.
[16] K. J. Vetter, *Z. Phys. Chem.* **196** (1951) 360–77.
[17] P. H. Tedesco, V. B. De Rumi and J. A. Gonzalez-Quintana, *J. Inorg. Nucl. Chem.* **29** (1967) 2813–17.
[18] C. F. Baes, *Inorg. Nucl. Chem.* **24** (1962) 707–20.
[19] G. M. Ritcey and A. W. Ashbrook, 'Solvent extraction: principles and appliation to process metallurgy', Elsevier, Barking, G.B. (1984).
[20] X. Meng, J. Zha and Z. Xu, International Solvent Extraction Conference, Munich, Preprints, **2** (1986) 223–30.
[21] K. H. Oehr, United States Patent 4 313 804 (1982).